

Reviewer 1 Comment 1: Sources of particle number. The authors calculate the particle number contributed by each source based on the corresponding mass (equation 1 in the paper). This is wrong for two reasons. First a significant fraction of the particle mass is secondary (sulfates, nitrates, secondary organic aerosol). When the secondary mass increases, the contribution of the corresponding source to particle number does not. Second, coagulation involves particles from different sources. It is not clear to which source the authors assign the particle resulting from the coagulation of two particles from different sources. Both of these problems are quite important for ultrafine particle number concentrations. The errors of this oversimplified approach should be estimated (at least for one period) with careful zero-out analysis (e.g., removing only the ultrafines and not the larger particles to avoid changes in the condensation and coagulation sinks). If the error is significant the corresponding part of the work should be redone or should be replaced with just a description of the contributions to emissions for different size ranges.

Response: We apologize that the methods to calculate particle number were not explained clearly in the first version of the paper. The model framework uses a moving sectional approach to conserve particle number and mass while letting particle radius increase due to condensation (Kleeman, Cass, and Eldering 1997). The method to calculate source contributions to number concentration is performed for each moving section individually. Number is explicitly conserved and correctly apportioned to sources in this algorithm.

Each particle source type / moving size bin includes an artificial tracer equal to 1% of the primary particle mass. The mass of this tracer is related to the number of particles by the equation

$$\text{Tracer\_source}_i * 100 = N\_source_i * 3.14159/6 * Dp\_bin * \text{density\_source}_i$$

This equation can be easily rearranged to solve for  $N\_source_i$  as a function of  $\text{Tracer\_source}_i$  in each size bin. Again, since the model uses a moving sectional approach, number and tracer mass are exactly conserved. Condensation/evaporation changes the particle diameter as semi-volatile components move on and off the particle but this does not change  $\text{Tracer\_source}_i$  or  $N\_source_i$ . The moving sectional approach greatly simplifies the source apportionment of particle number compared to other models that use fixed particle size bins with condensation / evaporation transferring material between bins.

Coagulation is fastest between very small particles and relatively large particles in the atmosphere. The net effect of coagulation is to remove ultrafine particles from the atmosphere as they collide and join the particles larger than 100 nm. This loss mechanism is accurately simulated in the model calculations. The rate of “self-coagulation” between two ultrafine particles that produces a particle still in the ultrafine particle size range is negligible at atmospherically relevant concentrations. Table 2 compares the timescale for 0.01  $\mu\text{m}$  particles coagulating with other 0.01  $\mu\text{m}$  particles and coagulating with 0.1  $\mu\text{m}$  particles based on size distributions measured in a typical suburban environment in a California city (see Figure 1). The coagulation timescale between two 0.01  $\mu\text{m}$  particles is 209 hrs (8.7 days) while the coagulation timescale between 0.01  $\mu\text{m}$  particles and 0.1  $\mu\text{m}$  particles is 4.4 hours. Therefore, self-coagulation between ultrafine particles smaller than 60 nm is much less significant than coagulation between ultrafine particles and larger particles (acting as a loss mechanism for ultrafine particles in the atmosphere).

Table 2 Time scale for coagulation between 0.01  $\mu\text{m}$  particles with 0.01  $\mu\text{m}$  particles and 0.1  $\mu\text{m}$  particles in a typical suburban environment in California. See Fig 1 for size distribution used for calculations.

Particle size	0.01	0.1
Coagulation Coefficient( $\text{cm}^3/\text{s}$ )	1.90E-09	2.50E-08
PM Number concentration ( $\#/\text{cm}^3$ )	1.40E+03	5.00E+03
timescale (hours)	208.9	4.4

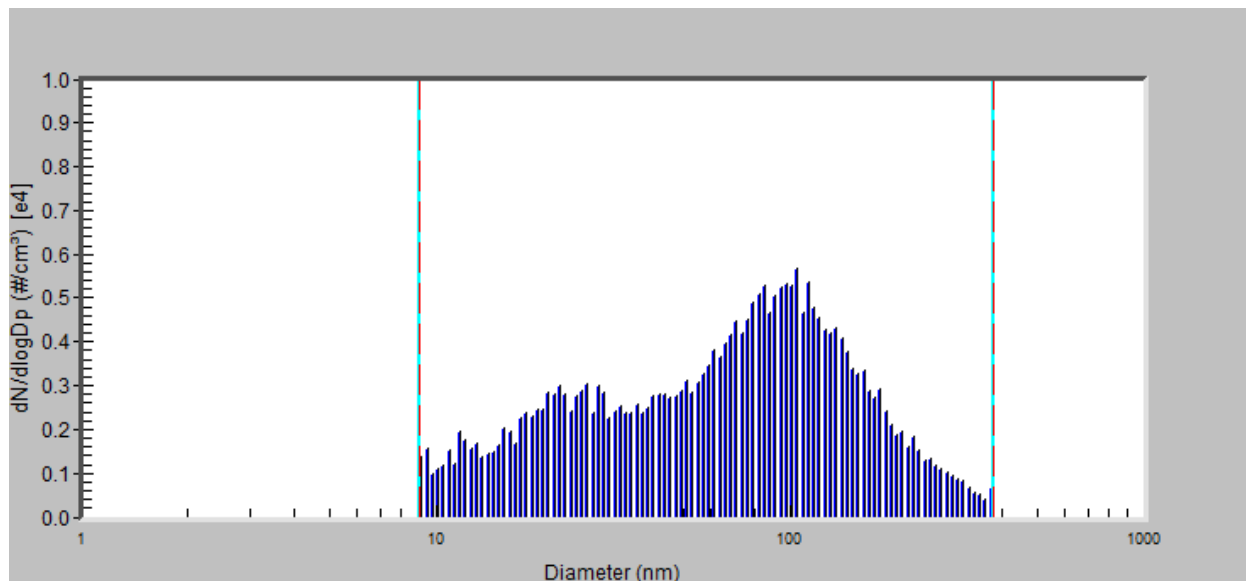


Figure 1 Particle size distribution measured in a typical suburban environment in a California city

Source apportionment calculations treat coagulation events between very small particles and very large particles in a manner analogous to condensation. When two particles coagulate, the mass of the smaller particle is added to the mass of the larger particle. The number concentration of the smaller particle is discarded while the number concentration of the larger particle stays constant. This slightly reduces the accuracy of source apportionment calculations for particle number in the larger size bins because the Tracer\_source mass in the larger size bin is no longer proportional to the number concentration from that source. This issue is relatively minor since size bins larger than  $1\mu\text{m}$  that act as the dominant sink during particle coagulation events typically account for less than 5% of the total number concentration.

Perturbation studies were conducted as requested by the reviewer by setting the UFP emissions for on-road gasoline vehicles to zero during the month August 2012. Emissions of gases and emissions of larger particles from on-road vehicles were not changed. The difference between this perturbation simulation vs. the basecase simulation was calculated to estimate the number concentration of particles associated with on-road gasoline vehicles. This “zero-out” concentration is then compared to the standard model source-apportionment calculations in Figure 2 below. The two methods for number source apportionment yield very similar spatial patterns and very similar maximum concentrations of approximately  $0.5 \text{ kcounts}/\text{cm}^3$ . The tracer source apportionment method accounts for all particle sizes

which produces slightly higher concentrations than the zero-out method that only considered particles smaller than 100 nm. This test confirms that the online source apportionment methods for number in the current study work correctly.

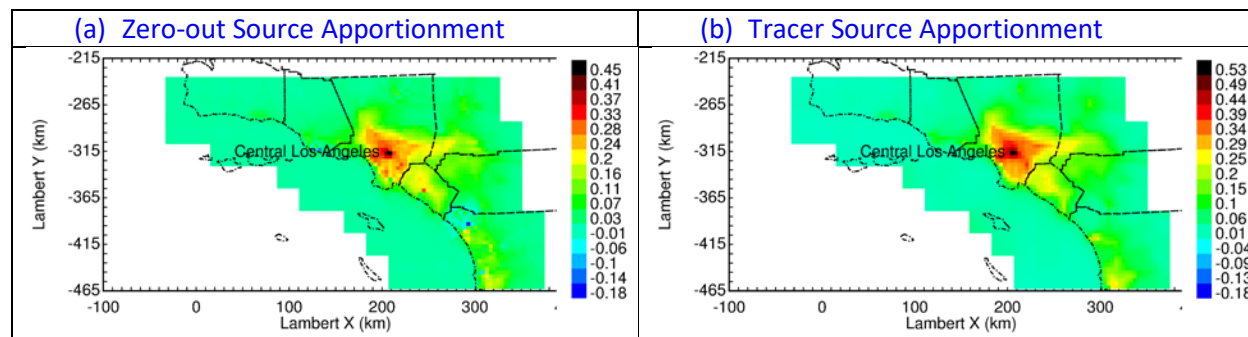


Figure 2 Particle number concentrations associated with on-road gasoline vehicles calculated using the zero-out method and the artificial tracer method in August 2012.

Reviewer 1 Comment 2: Importance of non-residential natural gas combustion as a source of ultrafine particles. This is clearly the most important, but also the most controversial finding of the study. The evidence provided to support this potentially very important result is rather weak and the authors miss a lot of opportunities to strengthen their argument.

The first is the use of size distributions. The predicted size distributions from this source apparently peak in the 10-20 nm size range. There are a lot of available size distribution measurements in the area that can be directly compared with the model predictions. My understanding however is that the measured number size distributions (not immediately next to freeways) peak at the 35-40 nm range (see for example Sowlat et al., 2016). Some of these size distribution measurements are available for the periods that have been simulated so a comparison of size distributions (including sources) could be performed without much effort.

The second is the use of the spatial distribution of particle number. The predicted concentration maps are not shown, but one would expect much higher concentrations near the corresponding major source areas. Traffic should have quite a different spatial pattern. There have been also a lot of particle number distribution measurements in California during the last decade. An effort to test if the predicted patterns match the observed ones would help.

The third is the average diurnal variation. However, this study assumes that the non-residential natural gas emissions have a similar temporal pattern as traffic (Figure S2). So the observed rush-hour peak in particle number that all previous studies assign to traffic, here is explained by natural gas combustion. However, more careful spatio-temporal analysis could help strengthen (or weaken) the conclusion. For example, the predicted morning number peak in Rubidoux in summer does not exist in the measurements. The situation is even worse in midday during the winter suggesting that emissions from this source are clearly overestimated in this area. Is this helpful? Is this area dominated by these emissions or is the sampling site an exception? On the other hand, the model performs well in other areas so one could make the opposite argument site by site. However, without using all the information about predicted patterns in space and time it is difficult to reach a conclusion.

Response: Xue et al. showed that the primary size distribution for natural gas combustion peaks at approximately 20 nm but the size mode grows to approximately 60 nm after 3 hrs of aging in a smog chamber with a representative urban atmosphere consistent of realistic concentrations of VOCs and NOx under realistic UV intensity (Xue et al. 2018). Similar growth occurs in model calculations meaning that the natural gas particles do not stay static at 20 nm in the atmosphere. The measurements of larger particles in the atmosphere therefore do not definitively identify sources. Expert opinion is still required to interpret the size distributions and assign them to sources. The results of the current study should help refine those expert opinions in the future.

Many of the spatial patterns measured for airborne particle number concentrations have focused on the gradients around roads (see for example (Zhang et al., 2005; Zhang et al., 2004; Zhu et al., 2002a; Zhu et al., 2002b)). Likewise, the study performed by Solwat et al. (2016) referenced by the reviewer was carried out within 150m of a major freeway and so the reported particle size distributions are dominated by traffic sources. These gradients are impossible to resolve using a regional model with 4km resolution. A limited set of additional simulations were conducted using the WRF/Chem model configured with Large Eddy Simulation (LES) around Oakland California so that spatial scales down to 250m could be examined. Maps of the predicted ultrafine particle mass concentrations for gasoline, diesel, food cooking, wood combustion, and natural gas combustion particles are shown in Figure 3 below. At 250m resolution, ultrafine particles from diesel engines peak on major transportation corridors while ultrafine particles from gasoline vehicles are more diffuse reflecting their increased activity on adjacent surface streets. Ultrafine particles from natural gas combustion are even more diffuse reflecting contributions from area sources across the region. As the spatial resolution decreases to 1km and then 4km, the fine details around roadways are artificially diluted in the larger grid cells. This process shifts the dominant source of ultrafine particles over roadways from diesel engines at 250m resolution to natural gas combustion at 4km resolution.

The ultrafine particle model simulations summarized in Figure 3 are consistent with measurements of particle number in the proximity of roadways which show that the traffic contribution to particle number concentration decays to background levels within 300 m (Zhu, Hinds, Kim, Shen, et al. 2002; Zhu, Hinds, Kim, and Sioutas 2002). The measurements made by Zhu et al. indicate that the traffic contribution to regional number concentration cannot be distinguished from other sources on a regional scale using 4km grid cells which is the focus of this study.

Repeating all of the simulations at 250m resolution is beyond the scope of the current study. We emphasize the regional scope of the simulations in the main text of the revised manuscript to inform the readers about the appropriate interpretation of the current results, and we have also added “regional” to the title of the manuscript.

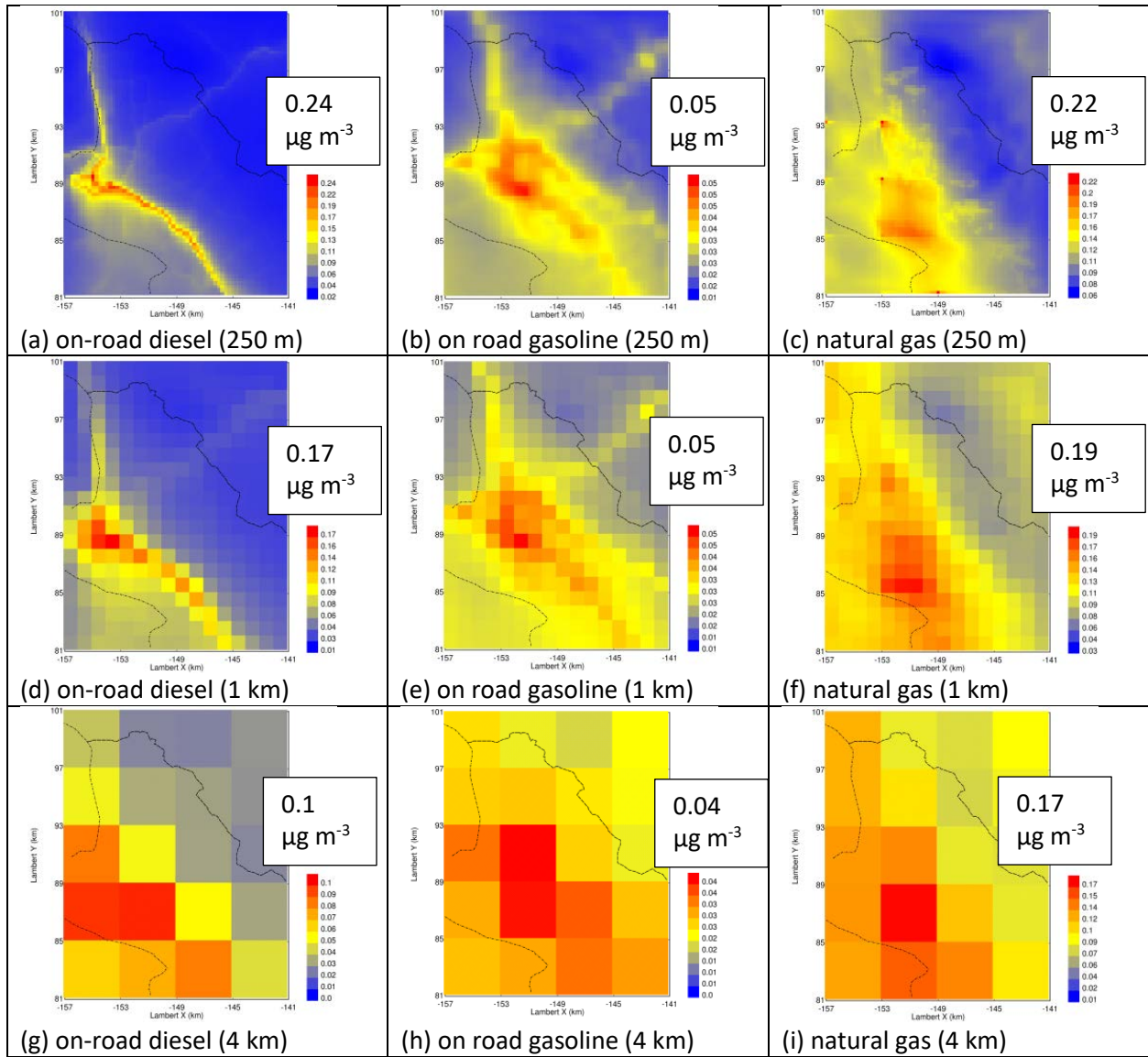


Figure 3:  $\text{PM}_{0.1}$  mass concentration associated with on-road diesel, on-road gasoline, and natural gas combustion at 250m, 1km, and 4km resolution over Oakland, California.

Hudda et al. (2014) found that particle number concentrations increased by a factor of four to eight downwind of the Los Angeles International Airport (LAX) based on measurements in June-July 2013. Total ground-level number concentrations in the LAX plume reached  $60\text{-}70 \times 10^3$  counts/cm<sup>3</sup>. Figure 4 illustrates the predicted number concentration associated with primary emissions (Figures 4a-i) and nucleation (Figure j) averaged over the months Aug-Dec 2012. Figure 4g shows that primary aircraft emissions in the LAX plume are predicted to account for  $8 \times 10^3$  counts/cm<sup>3</sup> and Figure 4j shows that nucleation of aircraft emissions in the LAX plume are predicted to account for  $45 \times 10^3$  counts/cm<sup>3</sup> yielding a total number concentration associated with LAX aircraft of approximately  $53 \times 10^3$  counts/cm<sup>3</sup>. Given the 4km spatial resolution of the model calculations, these findings are in good agreement with the measurements by Hudda et al. (2014).

It is noteworthy that military airbases in Figure 4g have significantly higher particle number concentrations due to their use of aviation fuel with higher sulfur content but nucleation plumes are not present downwind of these locations (Figure 4j). Particles emitted from military aircraft are represented as primary emissions in the current model calculations. Future measurements should compare particle number concentrations downwind of civilian and military airports to fully evaluate the impact of aviation fuel sulfur content on ambient ultrafine particle concentrations.

Figure 5 illustrates the predicted particle number concentrations associated with primary sources and nucleation in northern California. The relative importance of sources and the prediction of nucleation downwind of major sulfur emissions are consistent in northern and southern California. Natural gas combustion is a notable strong source of ultrafine particles in both regions due to the widespread use of this fuel in numerous residential, commercial, and industrial applications. In many cases, the natural gas combustion particles contribute strongly to the “urban background” concentrations over most California cities without the formation of individual plumes such as those found downwind of LAX. Future measurements could correlate ambient particle number concentrations and natural gas utilization across multiple cities to evaluate whether natural gas combustion is a significant source of particle number concentration.

The spatial patterns of particle number concentrations have been summarized in the main text of the revised manuscript.

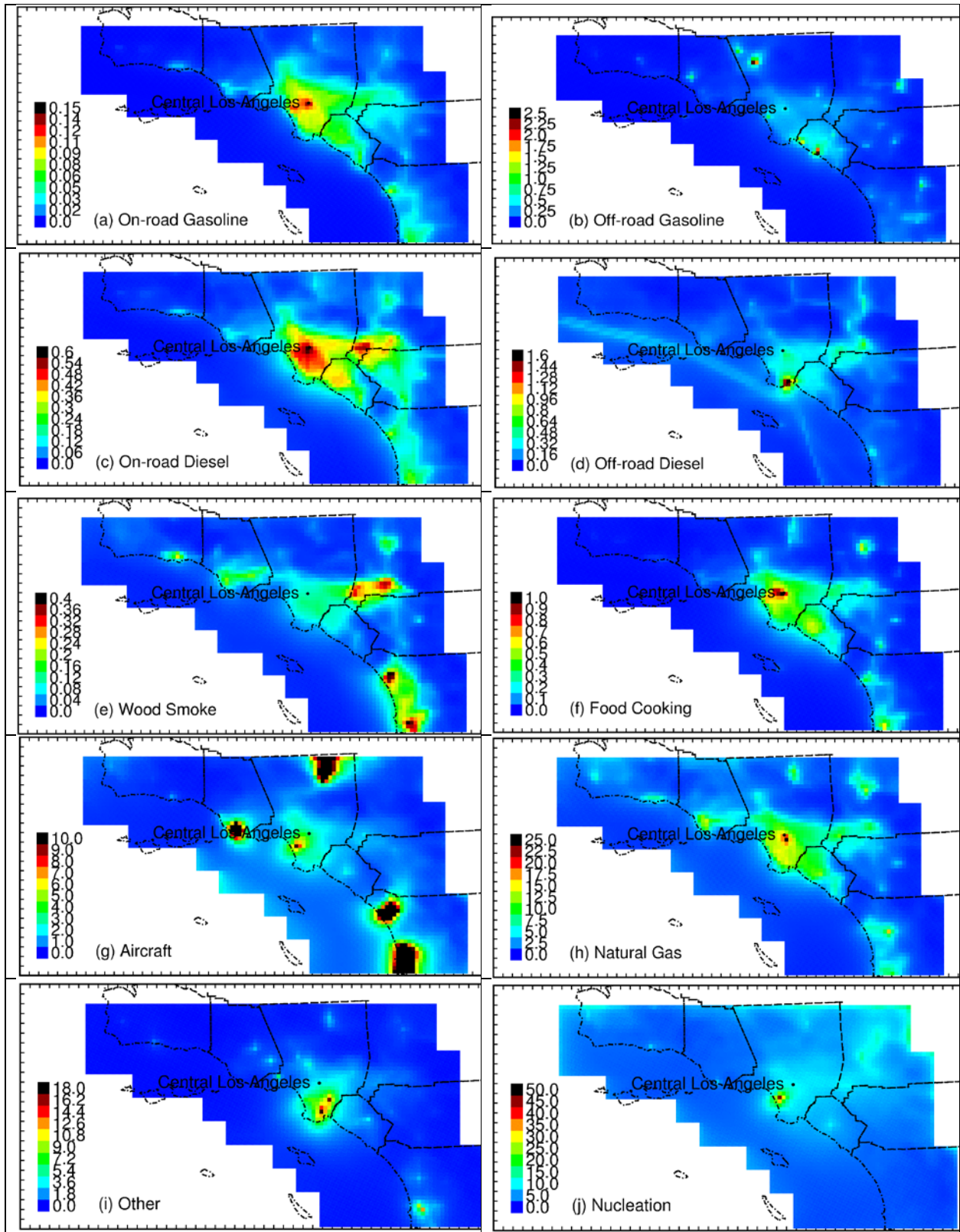


Figure 4. Spatial distribution of particle number from major sources in Southern California (unit: kcount/cm<sup>3</sup>).

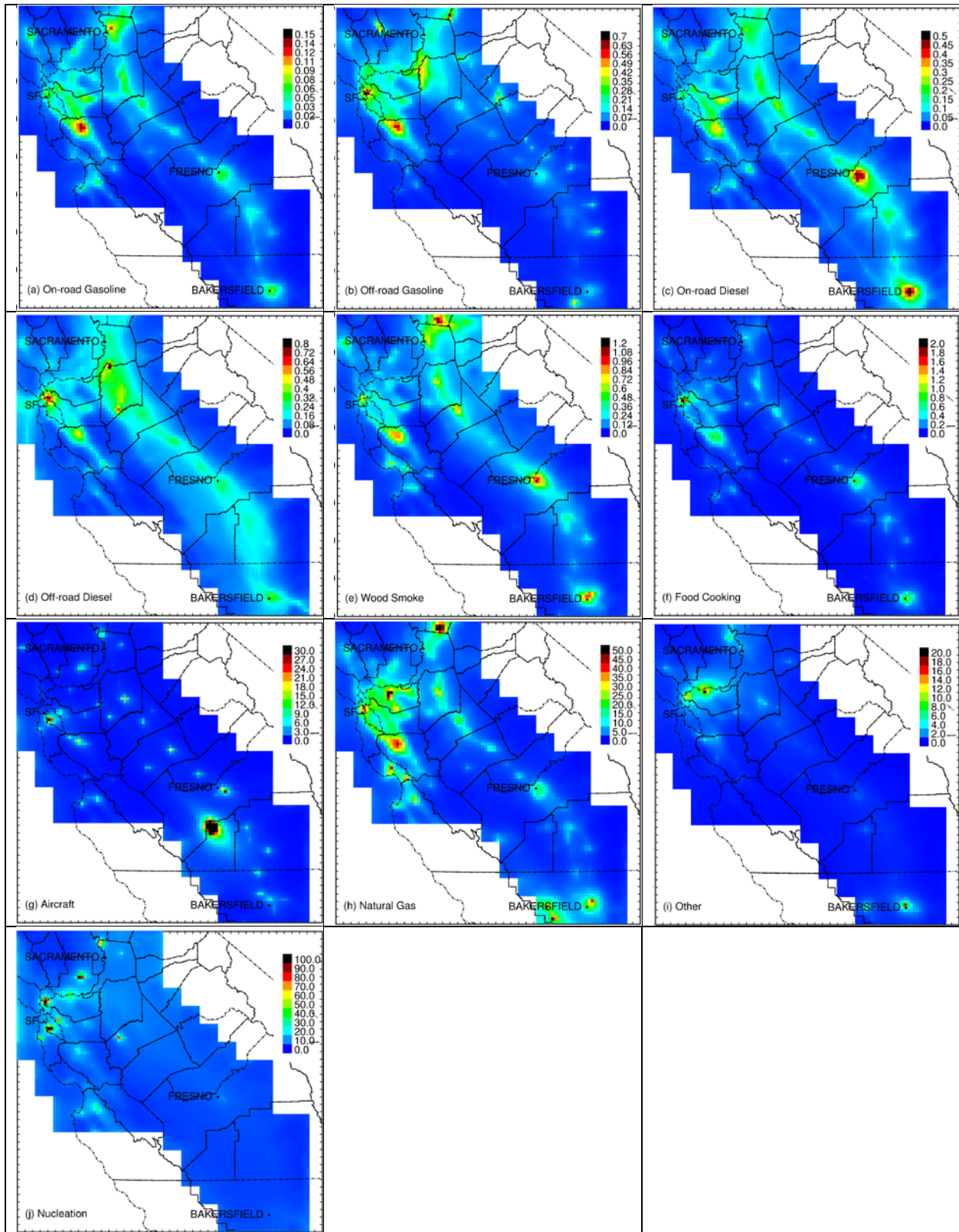


Figure 5. Spatial distribution of particle number from major sources in Northern California (unit: kcount/cm<sup>3</sup>).

The diurnal variation of the natural gas combustion emissions noted by the reviewer were obtained independently from the emissions inventory specified by the California Air Resources Board. The activity pattern is based on energy demand as a function of time of day. Both natural gas combustion and motor vehicle activity follow the diurnal cycle of human activity across California, with peaks in the early morning and late afternoon. The current model predictions suggest that natural gas combustion contributes strongly to this pattern.

We acknowledge that the model predictions match the measured particle trends at some locations but not as well in other locations. We are not claiming that the model is perfect, but we feel that the information available does suggest that natural gas combustion is a major regional source of ultrafine particles that has not been previously recognized.

Reviewer 1 Comment 3: Modeling of growth of ultrafine particles. The approach used to simulate condensation/evaporation of sulfuric acid, ammonium, nitric acid, secondary organics on the ultrafine particles in this study is not explained in any detail. There is a rather confusing statement in lines 129-137 that “dynamic condensation/evaporation is not considered”. Does this mean that the particles are assumed to be in equilibrium? If yes, how does the model deal with the effect of surface tension on the equilibrium vapor pressure especially in the 10-20 nm range? Do these particles evaporate because their equilibrium vapor pressure is higher than that of the bigger particles? This is a crucial process for the number concentration of the smaller particles and it is not clear that it is simulated properly.

Response: Dynamic simulation of the condensation/evaporation of ultrafine particles is a computationally expensive exercise (Zhang et al. 2004, 2005; Zhang and Wexler 2004). Some of the particles evaporate downwind of sources like freeways, while other particles grow due to the condensation mostly of secondary organic aerosol (Anttila and Kerminen 2003; Troestl et al. 2016). The most extreme changes to the particle size distribution occur within the first few min after emissions to the atmosphere (within 300 m of roadways), with more stable behavior over long time periods.

Regional grid models used to predict regional number concentrations are not well-suited to simulating the dynamic behavior of the near-source particle size distribution for the first few minutes after release to the atmosphere. Evaporation of UFPs near the source is therefore represented by reducing the primary emissions of nano-particles based on measurements conducted at high dilution factors (Xue et al. 2018) or using measurements of particle volatility to estimate the evaporation at high dilution factors (May, Levin, et al. 2013; May, Presto, et al. 2013; Kuwayama et al. 2015). These regionally-representative emissions provide the starting point for the model calculations.

The condensation of fresh sulfate, nitrate, ammonium ion, and SOA onto UFPs with diameters between 10 – 100 nm was simulated using the standard dynamic gas-particle partitioning methods in the model. These calculations do not change the predicted number concentration in the regional atmosphere. Condensation shifts the size distribution upward at a rate of approximately 2-3 nm hr<sup>-1</sup> under favorable conditions. This has been clarified in the revised manuscript.

Reviewer 2 Comment 1: Definition of particle number concentration. The use of the term particle number concentration throughout this paper is often confusing and sometimes misleading. It is important to always define the lower threshold of the size range of the corresponding concentration. The total particle concentration can be easily a factor of 2 or 3 higher than the concentration of particles with diameter higher than 10 nm (N10).

Response: We will revise the paper to use the term  $N_x$  throughout where X refers to the lower size cut of the measurements or model predictions. The term PNC will no longer be used.

Reviewer 2 Comment 2: Growth of freshly nucleated particles to 10 nm. The authors state that they parameterize the growth process following the work of Kerminen and Kulmala (2002). However, this parameterization requires the growth rate (GR) of the particles. The calculation of this rate is non-trivial in a model with coarse aerosol size resolution such as the current one. Errors in the GR can lead to significant errors in the estimation of the contribution of nucleation as a source to particle number. The authors should evaluate the error of this parameterization for their aerosol model.

Response: The growth rate (GR) in the Kerminen and Kulmala (2002) parameterization is one of the factors that accounts for the competition between the condensation and nucleation of over-saturated compounds until the nucleated particles grow to the size of the smallest bin in the regional model at which point this competition is represented explicitly by the model operators. In current study, we predicted the growth of the sulfate particles from nuclei using the equation

$$GR \approx \frac{3 \times 10^{-9}}{\rho_{nuc}} M_{sulf} u_{sulf} C_{sulf} \quad (\text{eq. 1})$$

following (Kerminen and Kulmala 2002). Here,  $\rho_{nuc}$  is the density of the nucleation mode sulfate particles which was set to be 1.77 kg m<sup>-3</sup> at 20°C, 1 atm;  $M_{sulf}$  is the molecular weight of nucleation mode sulfate particle which was set to be 98 g mol<sup>-1</sup>;  $C_{sulf}$  is the vapor concentration of sulfate (H<sub>2</sub>SO<sub>4</sub>); and  $u_{sulf}$  is temperature ( $T$ ) dependent molecular speed of the sulfate vapor which is calculated as follows, in m s<sup>-1</sup>.

$$u_{sulf} = \sqrt{\frac{3RT}{M_{sulf}}} \quad (\text{eq.2})$$

According to (Kerminen and Kulmala 2002), uncertainty associated with eq. 1 is minor. Perturbation studies were conducted in the current analysis with a box model configured to represent a single grid cell using the full set of model operators. The GR predicted by eq 1 was multiplied by a factor ranging from 0.5 to 2.0 to test the sensitivity of the model results. Initial conditions were 0.04 ppm O<sub>3</sub>, 0.05 ppm NO, 0.0 ppm NO<sub>2</sub>, 0.05 ppm HCHO, 0.1 ppm ISOPRENE, 0.1 ppm BENZENE, and 0.01 ppm ALK5. A nucleation event was initiated at 8am by setting H<sub>2</sub>SO<sub>4</sub> concentrations to 1e7 molecules cm<sup>-3</sup> and NH<sub>3</sub> concentrations to 100 ppt. Figure 6 illustrates the growth of nucleated particles between 5am and 12 noon for July in California. The number concentration of nucleated particles increases to values between 2500 - 3000 #/cm<sup>3</sup>. SOA condenses on the particles causing their size to increase above 100nm. Coagulation and deposition processes remove particles over time.

Three separate simulations are illustrated in Figure 6 using the nominal GR predicted by eq 1 along with perturbations of 0.5\*GR and 2.0\*GR. These model perturbations fall almost exactly on top of the basecase simulations, suggesting that results are not overly sensitive to GR during the first few seconds of nuclei growth before calculations are handed off to the regional model algorithms.

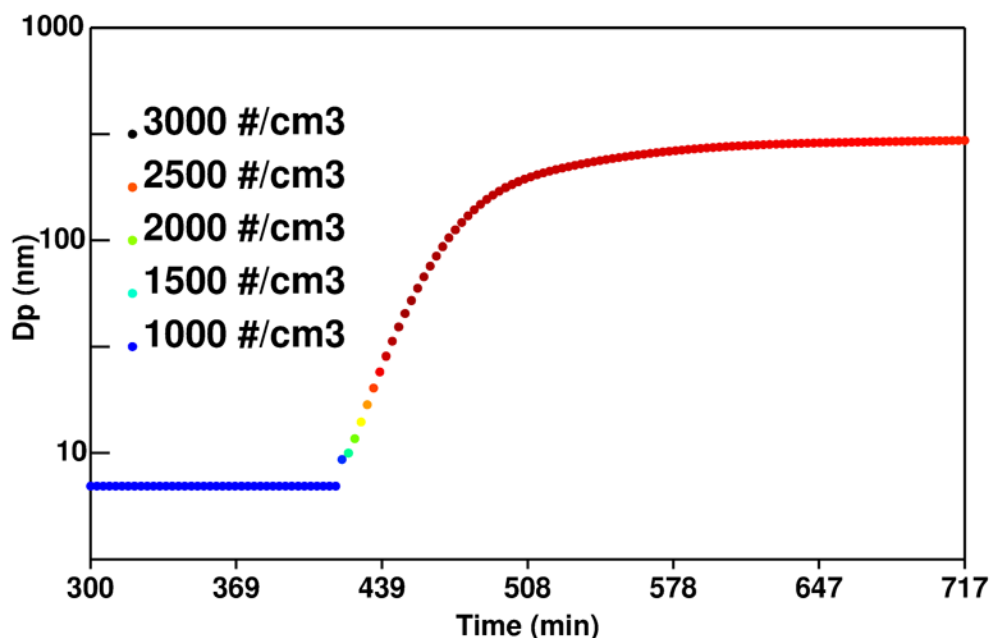


Fig 6: Simulated particle nucleation event followed by growth due to SOA condensation under conditions representing July in California. Vertical axis displays the mean diameter of the nuclei mode while color represents the particle number concentration.

Reviewer 2 Comment 3: There is little information provided about the frequency and spatial extent of nucleation in the simulations in the various seasons. This information is needed to understand the simulation results.

Response: The concentrations of nucleated particles in August, October, and December are shown in Figure 7 (Southern California) and Figure 8 (Northern California) below. Nucleation events occur in the regions where sulfur emissions are highest (typically airports, shipping ports and refining facilities). Concentrations of nucleated particles are higher in October and December than in August because colder temperatures increase nucleation rates if the precursor  $\text{H}_2\text{SO}_4$  and  $\text{NH}_3$  concentrations are relatively constant. A significant fraction of the  $\text{H}_2\text{SO}_4$  in the current simulation is produced by the fast conversion of gas-phase  $\text{SO}_3$  emissions to  $\text{H}_2\text{SO}_4$  in the exhaust plume near the emissions source.  $\text{SO}_3$  conversion does not depend on the presence of oxidants in the atmosphere and so the higher oxidant concentrations in the summer do not dominate the seasonal nucleation pattern.

Once  $\text{H}_2\text{SO}_4$  forms in the exhaust plumes, it either condenses onto existing particles formed from lower volatility compounds in the plume, or it mixes with  $\text{NH}_3$  in the background air and nucleates. This process is captured by dilution source sampling measurements that allow for a few minutes of aging time and so the size-resolved emissions profiles for many sources already account for the effects of nucleation within the “near-field” exhaust plume (within a few 10’s of meters after emission).  $\text{SO}_3$  emissions from reciprocating internal combustion engines were therefore set to zero to avoid double counting the new particle formation downwind of these sources in the current study. Regular  $\text{SO}_2$  emissions from these sources were not modified. Emissions from aircraft jet engines have high exit velocity which promotes rapid mixing with background air.  $\text{SO}_3$  emissions were left at their nominal levels (3-4% of total  $\text{SO}_x$ ) for jet engine aircraft in the current study. The consequence of these model

treatments is that predicted concentrations of nucleated particles are highest downwind of LAX, which agrees with measurements of ambient particle number concentrations (Hudda et al., 2014).

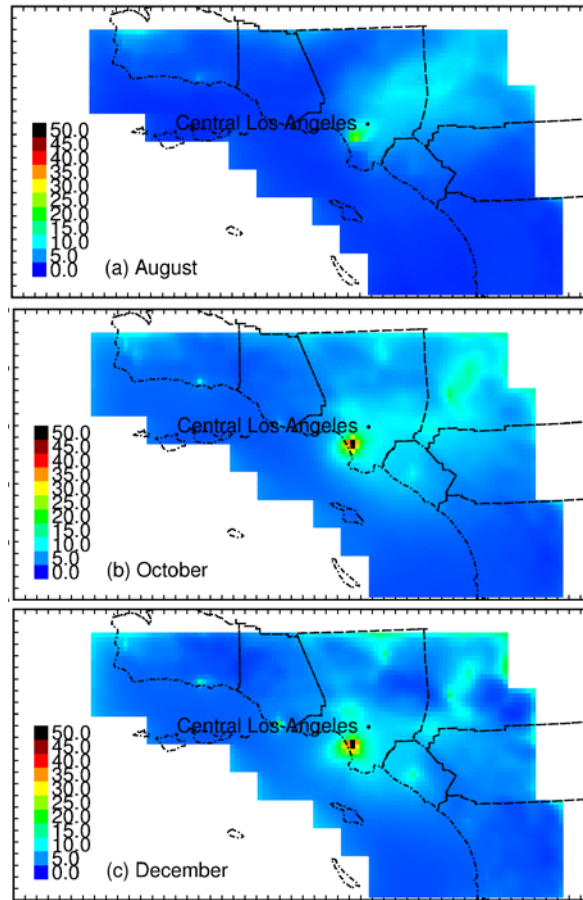


Figure 7: Seasonal variation of nucleated particle concentrations in Southern California. Units are  $\text{kcount}/\text{cm}^3$ .

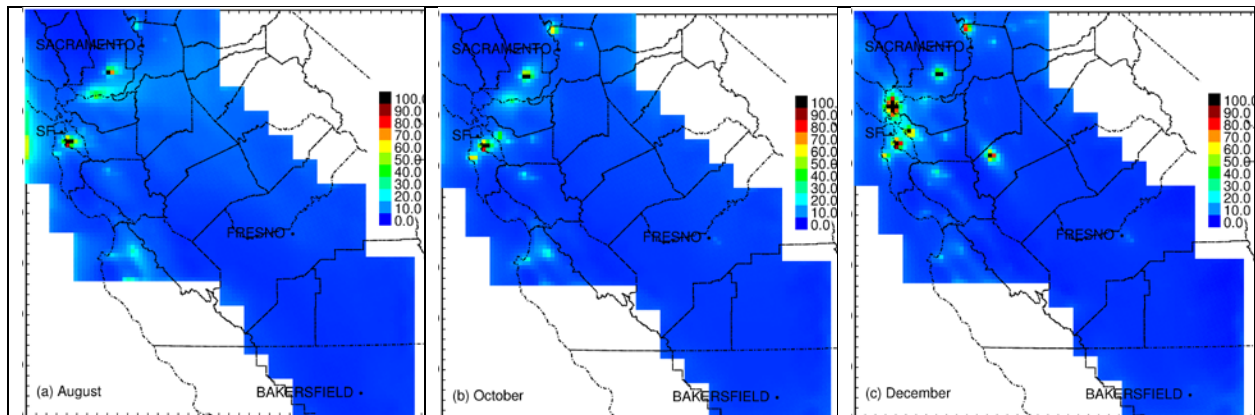


Figure 8: Seasonal variation of nucleated particle concentrations in Northern California. Units are  $\text{kcount}/\text{cm}^3$ .

Reviewer 2 Comment 4: Emissions from natural gas combustion. A map of the estimated N10 and PM0.1 emissions from this major source is needed (see also comment 1.2). Also the average diurnal profile of the emissions for the domain and the average size distribution should be shown.

Response: The map of emissions from natural gas sources are shown below. Note that particulate matter emissions from all natural gas sources other than reciprocating engines have been reduced by 70% to account for evaporation of particles after emission to the atmosphere (Xue et al. 2018). The average diurnal profile of the natural gas emissions for the domain is shown in Figure S2 and the average size distribution is shown in Figure S3 of the original manuscript.

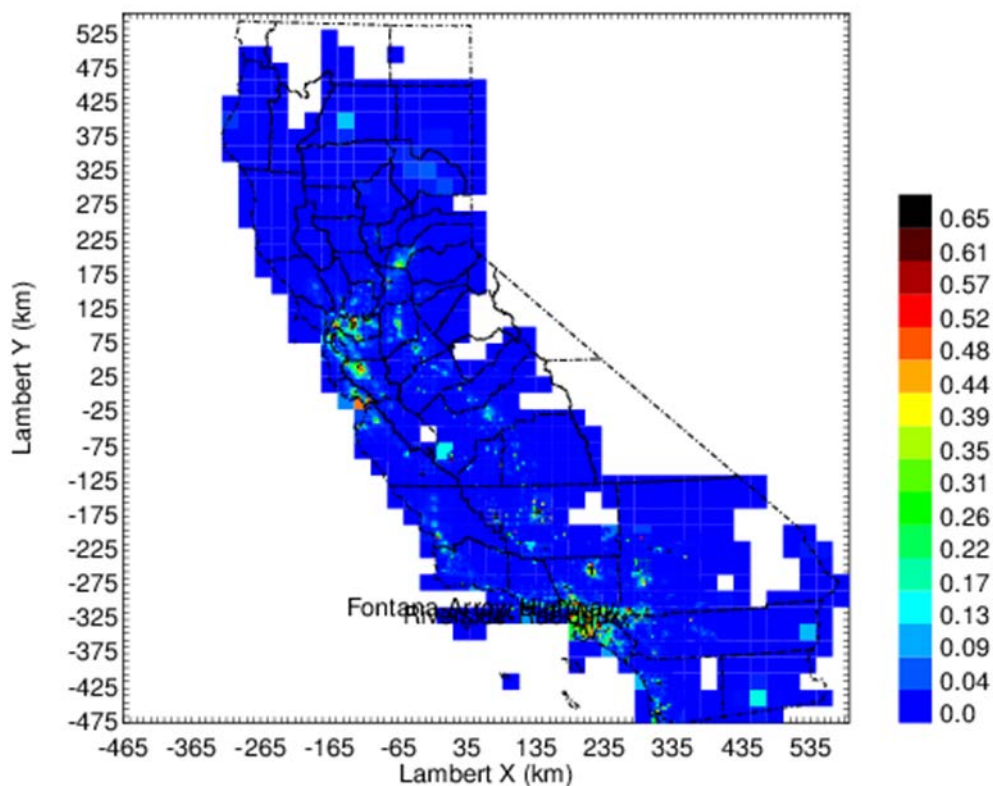


Figure 5. Daily average natural gas combustion emissions for California.

Reviewer 2 Comment 5: Temporal scale of evaluation. The authors present metrics of the model performance but they do not clarify if these are for hourly, daily, monthly, simulation averages or something else. The text and the corresponding tables do not include this information. Given the availability hourly measurements evaluation at this timescale should be also performed (if it has not been performed yet). The evaluation at a daily scale is also useful.

Response: Comparisons in the manuscript are based on daily averages which corresponds to the shortest averaging time that should be used for the current model results. Comparisons to measurements at hourly and daily time scales are shown in Figure 6 below for particle number

concentration. The hourly comparisons meet model performance criteria, but have slightly worse performance than the daily averages because the calculations do not fully capture all of the random variability in meteorological patterns and emissions patterns over hourly time scales. Further work would be required to create accurate model results at hourly time scales, but this effort is beyond the reasonable scope of the current study. We do not wish to present hourly-average performance metrics in the manuscript because we do not want to encourage the use of the model results at this time scale.

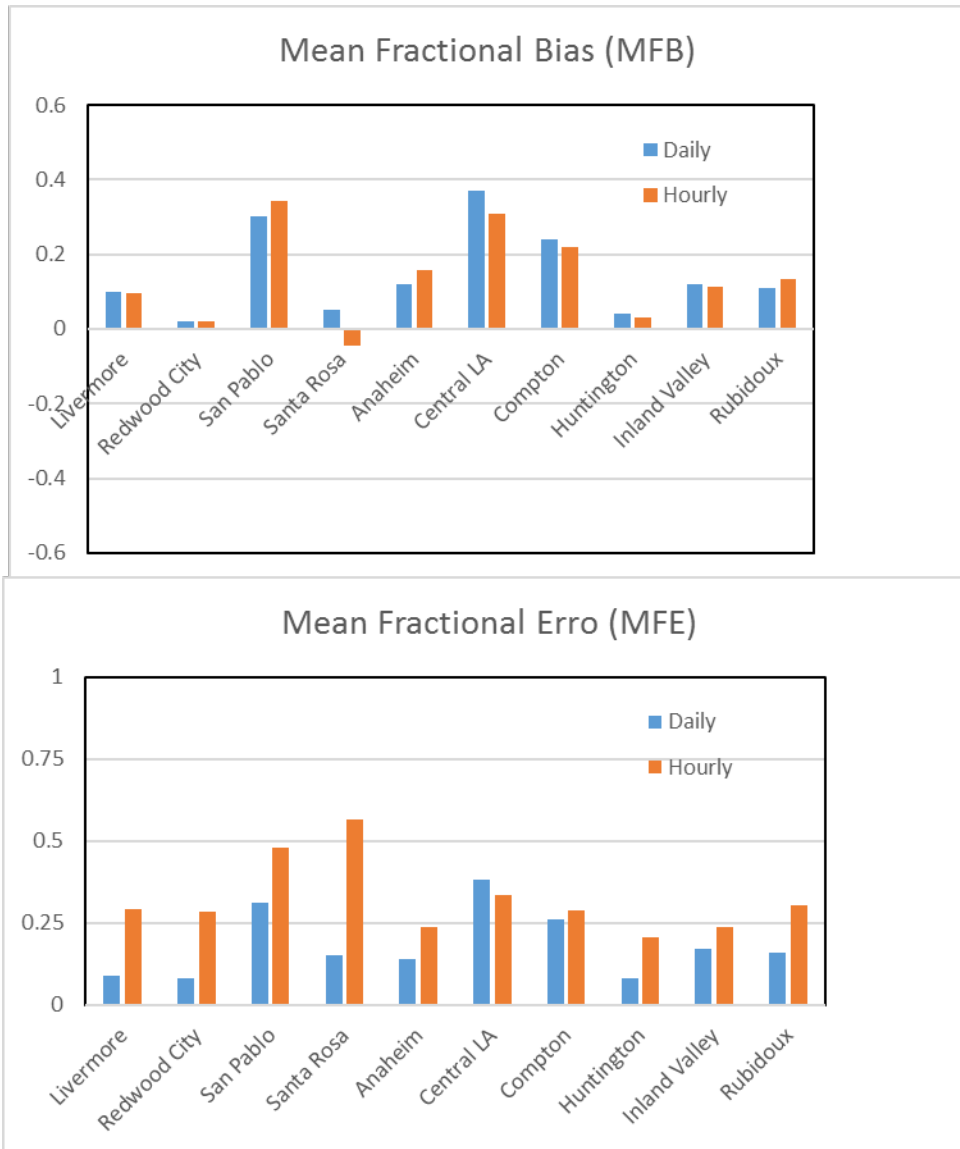


Figure 6 Mean Fractional Bias (MFB) and Mean Fractional Error (MFE) of N10 at 10 sites in California

Reviewer 2 Comment 6: The measurements of particle number refer to N6 and N7 while the predictions to N10. The authors suggest that the average error in the corresponding comparisons should be less than 10

Response: Yes, we feel that comparison between N6 to N10 will only introduce a small amount of uncertainty into the calculation. We would welcome recommendation from the reviewer to adjust the comparison to account for this size difference.

Reviewer 2 Comment 7: The use of qualitative terms (general agreement, agree reasonably well, good agreement) is not helpful and should be avoided.

Response: All qualitative statements will be removed in the final paper.

Reviewer 2 Comment 8: If my understanding of the paper is correct, the current model does not use the dynamic organic aerosol scheme used by Hu et al. (2017). If this is the case, the results regarding the contribution of SOA to PM<sub>0.1</sub> in this work should be discussed and should be compared to that version of the model. If it is the same it should be clearly stated.

Response: We apologize that the original text was not clearer. The current study uses the same dynamic organic aerosol scheme used by (Hu et al. 2017). This point will be clarified in the revised manuscript.

Reviewer 2 Comment 9: Contribution of traffic particles. Ronkko et al. (PNAS, 114, 7549-7554, 2017) argued that traffic is an even more important source of particle number, because there are a lot of sub-10 nm particles emitted. Given that the current study does not include primary traffic particles smaller than 10 nm (which of course can grow to larger sizes), can it seriously underestimate the contribution of this source in urban environments?

Response: The [measurements](#) in the roadside environment consistently show that traffic dominates nano-particle concentrations. But the [measurements](#) moving downwind of the roadside environment show that these traffic nano-particles evaporate and do not increase the urban particle number concentration at distances more than 300 m downwind of the roadway (Zhu, Hinds, Kim, Shen, et al. 2002; Zhu, Hinds, Kim, and Sioutas 2002). This is a [measurement](#) conclusion based on independent work not associated with the current manuscript, but it supports the methods used to represent traffic in the regional calculations.

Reviewer 3 Comment 1: The abstract says that simulations have been performed for 2012, 2015 and 2016. However, the presented results are only for 2012. This is important because there are available size distribution measurements for 2015-16 in the modeling domain that can be used for the evaluation of the model predictions (see comment 1.2).

Response: Figures 2 and 3 show the results of the model predictions to CMB results for 2015 and 2016. These findings were added to show that the predictions for PM<sub>0.1</sub> traffic contributions are in good agreement with measurements, supporting the accuracy of the predictions for the relative importance of traffic vs. other sources of UFP.

The additional particle number concentration measurements in 2015-16 that could be added to the manuscript are the same type as those shown for 2012. All the number count measurements are for sites in the San Francisco Bay Area and Southern California that show essentially the same picture as the plots already included in the manuscript. A separate manuscript is under preparation showing comparisons to all available measurements from 2000-2016. We would like to present the full set of comparisons in a single manuscript rather than further fragmenting this dataset.

Reviewer 3 Comment 2: The predicted correlations between PM2.5 and particle number concentrations can be compared with the corresponding measured correlations as an indirect way to evaluate the model performance.

Response: Table 3 below summarizes the predicted correlations between daily-average particle number concentrations and PM2.5 along with the measured correlations for these metrics. Measured correlations ( $R^2$ ) are less than 0.25 at all locations except Santa Rosa where correlations are above 0.5. Model predictions for daily-average particle number concentrations and PM2.5 are more highly correlated, with  $R^2$  ranging from 0.22 to 0.73. Locations with high  $R^2$  values such as central Los Angeles also have the highest MFB and MFE and so the high correlation between particle number and PM<sub>2.5</sub> may reflect inaccuracies in the model inputs. At other locations where traditional model performance metrics suggest that predictions are more accurate, the high correlation between particle number and PM<sub>2.5</sub> may be related to the model grid resolution. The 4km grid resolution used in the calculations smooths the sharp spatial gradients in the ultrafine particle concentration fields (see Response Figure 3). This same issue makes it difficult for point source measurements to accurately represent 4km average number concentrations. The particle number concentrations measured at a fixed monitoring location may not represent the variation in particle number concentrations a few km away. PM<sub>2.5</sub> concentration gradients are smoother, making model predictions and point measurements easier to compare. This analysis suggests that the model results contained in the current manuscript identify several important sources of ultrafine particles, but more work will be required to fully evaluate these results and possibly further refine the population exposure calculations.

Table 3. Daily-average correlation ( $R^2$ ) between PM2.5 mass and particle number concentration at 8 sites in California.

$R^2$	Livermore	Redwood City	San Pablo	Santa Rosa	Anaheim	Central LA	Compton	Rubidoux
Obs	0.04	0.01	0.16	0.58	0.08	0.14	0.15	0.22
Sim	0.28	0.49	0.55	0.22	0.51	0.73	0.61	0.50

Reviewer 3 Comment 3: Lines 66-67 “when nucleation algorithms were not standardized”. This statement is confusing.

Response: Will be changed to “...when different nucleation algorithms were used”.

Reviewer 3 Comment 4: Are the sulfate and nitrate concentrations shown in Table S4 for PM2.5 or for another size range?

Response: PM2.5

Reviewer 3 Comment 5: Table 1 should probably also include the predicted and measured average number concentrations.

Response: Revised Table 1 shown below.

	Ave Obs. Particles cm-3	Ave Sim. Particles cm-3	MFB	MFE	RMSE Particles cm-3
Livermore	8219	9201	0.10	0.09	3615
Redwood city	11500	11325	0.02	0.08	1132
San Pablo	10481	15822	0.30	0.31	10302
Santa Rosa	8655	8967	0.05	0.15	2063
Anaheim	12850	14812	0.12	0.14	4239
Central LA	17378	25376	0.37	0.38	10328
Compton	16203	21036	0.24	0.26	8127
Huntington	23207	24103	0.04	0.08	3698
Inland-Valley	15028	16875	0.12	0.17	4290
Rubidoux	10728	11920	0.11	0.16	3069

Reviewer 3 Comment 6: The terms “measured” and “predicted” should be used everywhere in Section 3.2.1 and other parts of the paper in which predictions are compared to measurements.

Response: This change will be made as suggested to the degree possible, but the term “measured” is too simplistic. The molecular marker measurements feed into a model prediction using the Chemical Mass Balance (CMB) model that has many model inputs and assumptions. There are no direct measurements of source contributions to PM0.1 – just model predictions using different techniques.

Reviewer 3 Comment 7: The number of samples and their duration corresponding to the results of Figs. 2-3 should be stated in the caption.

Response: Monthly average samples constructed from 3-day average measurements. This information will be added to figure caption as requested.

Reviewer 3 Comment 8: Line 296. Figures 4-6 and 7-9 do not show the seasonal variation of the corresponding variables. They show data (are these daily averages or something else) for different days in different seasons. These figures could be improved if they were split in four parts for the different periods simulated. The discussion could also be improved if the actual seasonal averages were shown (may be in the SI) and discussed.

Response: Figures show daily variation over months that span multiple seasons. The x-axis on each figure will be improved to show the months more clearly. Figure captions will be expanded to better explain the results.

Reviewer 3 Comment 9: Figure S2. What is A, B, and C? What is the average pattern in the domain?

Response: A, B and C represent different diurnal profiles used for different natural gas sources or regions based on information supplied by the California Air Resources Board. The average diurnal profile will be added to Figure S2.

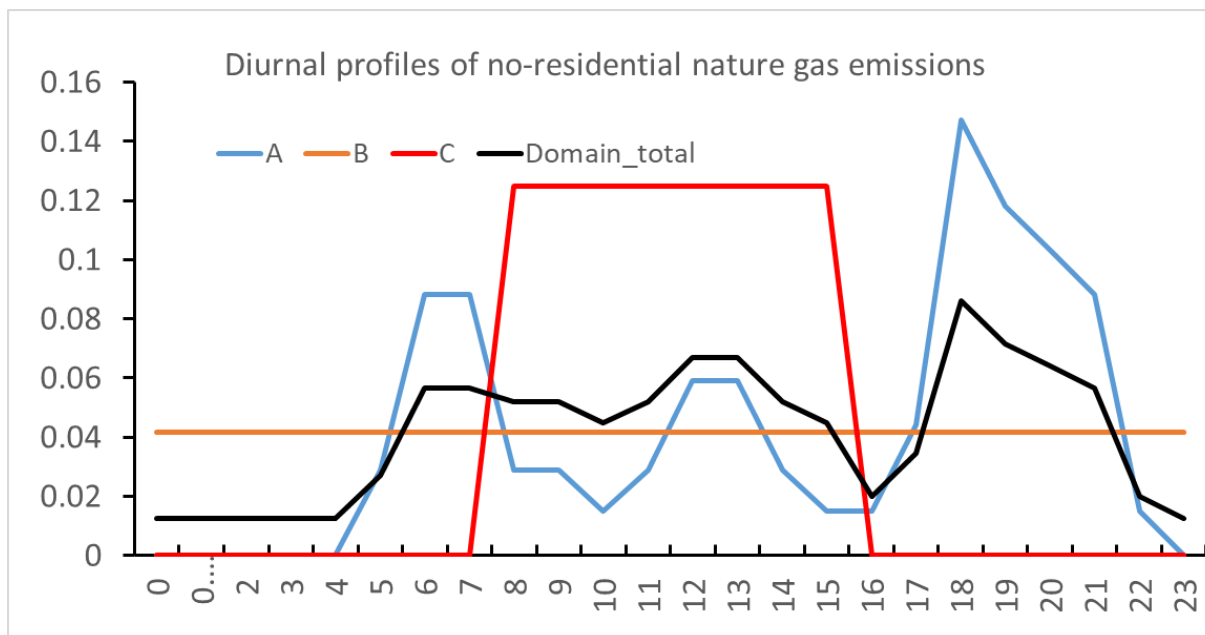


Figure S2 Diurnal profiles of no-residential natural gas emissions. A, B and C represents different types of diurnal profiles applied to natural gas emissions in the model. Black curve represents the average pattern in the domain.

#### References

Hudda, N., Gould, T., Hartin, K., Larson, T. V., and Fruin, S. A.: Emissions from an International Airport Increase Particle Number Concentrations 4-fold at 10 km Downwind, *Environmental science & technology*, 48, 6628-6635, 10.1021/es5001566, 2014.

Zhang, K. M., Wexler, A. S., Zhu, Y. F., Hinds, W. C., and Sioutas, C.: Evolution of particle number distribution near roadways. Part II: the 'road-to-ambient' process, *Atmospheric Environment*, 38, 6655-6665, 10.1016/j.atmosenv.2004.06.044, 2004.

Zhang, K. M., Wexler, A. S., Niemeier, D. A., Zhu, Y. F., Hinds, W. C., and Sioutas, C.: Evolution of particle number distribution near roadways. Part III: Traffic analysis and on-road size resolved particulate emission factors, *Atmospheric Environment*, 39, 4155-4166, 10.1016/j.atmosenv.2005.04.003, 2005.

Zhu, Y. F., Hinds, W. C., Kim, S., Shen, S., and Sioutas, C.: Study of ultrafine particles near a major highway with heavy-duty diesel traffic, *Atmospheric Environment*, 36, 4323-4335, 10.1016/s1352-2310(02)00354-0, 2002a.

Zhu, Y. F., Hinds, W. C., Kim, S., and Sioutas, C.: Concentration and size distribution of ultrafine particles near a major highway, *Journal of the Air & Waste Management Association*, 52, 1032-1042, 10.1080/10473289.2002.10470842, 2002b.